

Parton distribution functions and transverse momentum dependence of heavy mesons

Fernando E. Serna,¹ Bruno El-Bennich,^{2,3} and Gastão Krein³

¹*Departamento de Física, Universidad de Sucre, Carrera 28 No. 5-267, Barrio Puerta Roja, Sincelejo, Colombia*

²*Departamento de Física, Universidade Federal de São Paulo, Rua São Nicolau 210, Diadema, 09913-030 São Paulo, Brazil*

³*Instituto de Física Teórica, Universidade Estadual Paulista, Rua Dr. Bento Teobaldo Ferraz, 271 – Bloco II, 01140-070 São Paulo, SP, Brazil*

(Dated: September 4, 2024)

The leading Fock state light-front wave functions of heavy quarkonia and D and B mesons are obtained from the projections of their Bethe-Salpeter wave functions on the light front. We compute therefrom their leading-twist time-reversal even transverse momentum distributions and parton distribution functions. Mirroring the behavior of parton distribution amplitudes, the support of both distributions is increasingly narrower and shifted towards larger x as a function of the meson mass. The dependence of x and \mathbf{k}_\perp^2 of the transverse distributions does not factorize into separate functions, and their fall-off with \mathbf{k}_\perp^2 is much slower than that of light mesons.

I. INTRODUCTION

The definition of Light-Front Wave Functions (LFWFs) plays a fundamental role in the light-front quantization approach to Quantum Chromodynamics (QCD) [1], where they are essential objects that encode the nonperturbative internal dynamics of hadronic bound states. They provide a frame-independent representation of hadrons and a unique perspective on the *longitudinal and transverse* dynamics of their constituents. One can derive probability amplitudes from them, which describe the probability of finding partons, quarks and gluons, with a given longitudinal fraction of the hadron's total momentum as well as their transverse momentum dependence. Two of these distributions, the parton distribution function (PDF) and transverse momentum distribution (TMD), define hadronic operators that relate the partons to measurable hadronic observables [2–5], as they are experimentally accessible and provide valuable insights into the internal structure of hadrons.

From the perspective of continuum QCD and its application to hadron phenomenology, a LFWF provides a starting point to compute generalized parton distributions, form factors, structure functions, and gravitational form factors. On the other hand, since the light front is not directly accessible in nonperturbative approaches formulated in Euclidean space, the calculation of a hadron's LFWF poses a challenge. This is certainly the case in lattice-regularized QCD and with functional methods in continuum QCD, and has prompted alternative approaches to solving light-front quantized field theories directly [6, 7], for instance with a large momentum expansion of the equal-time Euclidean correlation functions in instant quantization [8] or with the projection of the Bethe-Salpeter wave function on the light front [9, 11].

The latter approach has recently been pursued to extract the LFWF from an Euclidian wave function computed within the combined framework of the Dyson-Schwinger equation (DSE) and Bethe-Salpeter equation

(BSE) [10] and to compute the PDF and TMD of light pseudoscalar and vector mesons [11–14]. Likewise, the LFWFs of D and B mesons were extracted from Mellin moments using an algebraic ansatz for the Bethe-Salpeter wave function in Ref. [15]. Herein, we fill a gap and extend these studies to the LFWF of D , D_s , B , B_s and B_c mesons with a DSE-BSE calculation that preserves the axialvector Ward identity [16–21]. With the wave functions, we then compute the meson's TMD and PDF.

II. LIGHT FRONT WAVE FUNCTIONS

The minimal $\bar{q}q$ Fock-state configuration of a pseudoscalar meson in light-front QCD is given by [3],

$$|M(P)\rangle = |M(P)\rangle_{|l_z|=0} + |M(P)\rangle_{|l_z|=1}. \quad (1)$$

The two states are described by two independent LFWFs, namely $\psi_0(x, \mathbf{k}_\perp^2)$ for the angular projection $l_z = 0$ and $\psi_1(x, \mathbf{k}_\perp^2)$ for $|l_z| = 1$, where \mathbf{k}_\perp is the transverse momentum and $x = k^+/P^+$ is the light-front momentum fraction of the quark. In a frame where the meson's transverse momentum vanishes, $\mathbf{P}_\perp = 0$, the transverse momentum of the antiquark is $\bar{\mathbf{k}}_\perp = -\mathbf{k}_\perp$ and its light-front momentum fraction is $\bar{x} = 1 - x$. The light-front components of a Euclidean four-vector $k_\mu = (k_1, k_2, k_3, k_4)$ are defined by $k^\pm = ik_4 \pm k_3$ and in terms of a light-like vector, $n^2 = 0$, we have $k^+ = n \cdot k$. Finally, the transverse momentum of the quark is defined by $\mathbf{k}_\perp = (k_1, k_2)$.

Starting from the matrix element definitions of the LFWFs, one can show that the pion's minimal Fock-state LFWFs is obtained from its Bethe-Salpeter wave function $\chi_M(k, P)$, with the two projections [9],

$$\begin{aligned} \Psi_{l_z}(x, \mathbf{k}_\perp^2) = & \sqrt{3}i \int \frac{dk^+ dk^-}{2\pi} \delta(xP^+ - k_\eta^+) \\ & \times \text{Tr}_D [\mathcal{O}_{l_z}^{+5} \chi_M(k, P)], \end{aligned} \quad (2)$$

where $\mathcal{O}_{l_z=0}^{+5} = \gamma^+ \gamma_5$ and $\mathcal{O}_{|l_z|=1}^{+5} = -i\sigma_{+i} k_\perp^i \gamma_5 / \mathbf{k}_\perp^2$ and the trace is over Dirac indices. The Bethe-Salpeter wave

function is defined by

$$\chi_M(k, P) = \int d^4z e^{-ik \cdot z} \langle 0 | \mathcal{T} f(z) \bar{g}(0) | M(P) \rangle, \quad (3)$$

and can be expressed as,

$$\chi_M(k, P) = S_f(k_\eta) \Gamma_M^{fg}(k, P) S_g(k_{\bar{\eta}}), \quad (4)$$

with the relative and total momenta k and P , respectively. The momenta of the dressed quark propagators $S_f(k_\eta)$ of given flavor f , $k_\eta = k + \eta P$ and $k_{\bar{\eta}} = k - \bar{\eta} P$, define momentum-fraction parameters: $\eta + \bar{\eta} = 1$. We recall that observables cannot depend on them due to translational invariance. The Bethe-Salpeter amplitude (BSA) of a pseudoscalar meson made of a quark f and antiquark g is generally defined as [22],

$$\begin{aligned} \Gamma_M^{fg}(k; P) = & \gamma_5 \left[i E_M^{fg}(k, P) + \gamma \cdot P F_M^{fg}(k, P) \right. \\ & \left. + \gamma \cdot k G_M^{fg}(k, P) + \sigma_{\mu\nu} k_\mu P_\nu H_M^{fg}(k, P) \right]. \end{aligned} \quad (5)$$

The wave functions $\chi_M(k, P)$ of pseudoscalar mesons, in particular of heavy-light bound states, are discussed in Refs. [18, 21] and we refer to details therein. They are obtained in the DSE and BSE framework with a self-consistent solution of the quark gap equation [23], which yields the dressed quark propagator for a given flavor, and of the homogeneous BSE, which gives the BSA of the meson. Our numerical solutions, however, are in Euclidean space where do not have direct access to objects defined on the light front. We use the following strategy to derive the LFWF from the Euclidean-space wave functions: we compute \mathbf{k}_\perp^2 -dependent moments of the LFWF defined by,

$$\langle x^m \rangle_{l_z}(\mathbf{k}_\perp^2) = \int_0^1 dx x^m \Psi_{l_z}(x, \mathbf{k}_\perp^2), \quad (6)$$

from which one can reconstruct the wave function on the domain $x \in [0, 1]$ and $\mathbf{k}_\perp^2 \in [0, \Lambda_\perp^2]$. Using Eq. (2) and integrating over the Dirac function, one finds,

$$\begin{aligned} \langle x^m \rangle_{l_z}(\mathbf{k}_\perp^2) = & \frac{\sqrt{3}i}{|P^+|} \int \frac{dk^+ dk^-}{2\pi} \left(\frac{k^+}{P^+} \right)^m \\ & \times \text{Tr}_D [\mathcal{O}_{l_z}^{+5} \chi_M(k, P)]. \end{aligned} \quad (7)$$

To facilitate the calculation of the moments defined by Eq. (7), we use an accurate parametrization of numerical solutions to the quark DSE and BSAs in rainbow-ladder truncation. We implement a complex conjugate pole parametrization (ccp) for the quark propagator defined by [24, 25]:

$$S_f(q) = \sum_{k=1}^N \left[\frac{z_k^f}{i\gamma \cdot q + m_k^f} + \frac{(z_k^f)^*}{i\gamma \cdot q + (m_k^f)^*} \right], \quad (8)$$

where m_k^f and z_k^f are complex numbers. These parameters are fitted to the numerical DSE solution for the

quark propagator with $N = 2$ on the real space-like axis $p^2 \in [0, \infty)$. The set of parameters for each flavor of quarks are reported in Ref. [18].

With respect to the BSA defined by Eq. (5), the scalar amplitudes $\vec{F} = (E_M, F_M, G_M, H_M)$ are parametrized by a Nakanishi type of integral representation [12] that allows a simultaneously fit of even and odd components of the BSA under $k \cdot P \rightarrow -k \cdot P$ and therefore of equal-mass as well as flavored mesons:

$$\mathcal{F}_i(k, P) = \sum_{j=1}^3 \int_{-1}^1 d\alpha \rho_j(\alpha) \frac{U_j \Lambda^{2n_j}}{(k^2 + \alpha k \cdot P + \Lambda^2)^{n_j}}. \quad (9)$$

The spectral densities $\rho_j(\alpha)$ are defined as $\rho_1(\alpha) = \rho_2(\alpha) = \rho_i(\alpha)$ and $\rho_3(\alpha) = \rho_u(\alpha)$ with

$$\rho_i(\alpha) = \frac{\Gamma(3/2)}{\sqrt{\pi} \Gamma(1)} \left[1 + \sum_{n=1}^3 \sigma_n C_n^{(1/2)}(\alpha) \right], \quad (10)$$

$$\rho_u(\alpha) = \frac{3}{4}(1 - \alpha^2), \quad (11)$$

where $C_n^{(1/2)}(\alpha)$ are Gegenbauer polynomials of order $1/2$. The scalar amplitude $H(k, P)$ is negligibly small and therefore neglected. The parameter sets of Eq. (9) are listed in the Appendix A.

With the numerical values for the transverse-momentum dependent moments (7) at hand, one can reconstruct the meson's LFWF. In order to do so, we need an algebraic parametrization for $\Psi_{l_z}(x, \mathbf{k}_\perp^2)$ which allows us to reconstruct it by comparison of the calculated moments $\langle x^m \rangle_{l_z}(\mathbf{k}_\perp^2)$ (7) with the ones using the definition in Eq. (6). Motivated by the algebraic model described in Ref. [15], we implement the following parametrization for the LFWF:

$$\Psi_{l_z}^{\text{rec.}}(x, \mathbf{k}_\perp^2) = \mathcal{N}_M \frac{\Delta_M^{2n}}{(\mathbf{k}_\perp^2 + \Delta_M^2)^{n+1}} \phi_M(x, \alpha, \beta), \quad (12)$$

where we fix $n = 4$ for all mesons and define the function,

$$\Delta_M^2(x) = \Lambda_1^2 + x(x-1)m_M^2 + x(\Lambda_2^2 - \Lambda_1^2). \quad (13)$$

\mathcal{N}_M , α , β , Λ_1 and Λ_2 are unknown scale-dependent parameters to be determined in the reconstruction process, while m_M is the ground-state mass eigenvalue of the meson that corresponds to the BSA (5). For the Light-Front Distribution Amplitude (LFDA), $\phi_M(x, \alpha, \beta)$, we employ the parametrization [20],

$$\phi_L(x, \alpha, \beta) = x^\alpha \bar{x}^\beta, \quad (14)$$

for light pseudoscalar mesons and

$$\phi_H(x, \alpha, \beta) = 4x\bar{x} e^{-4\alpha x\bar{x} - \beta(x-\bar{x})}, \quad (15)$$

for the heavy-light mesons and quarkonia with $\bar{x} = 1 - x$.

Finally, we reconstruct the LFWFs by minimizing the sum,

$$\epsilon(\mathcal{N}_M, \Lambda_1, \Lambda_2, \alpha, \beta) = \sum_{m=0}^{m_{\max}} \left| \frac{\langle x^m \rangle_{L,H}^{\text{rec.}}}{\langle x^m \rangle_{l_z}} - 1 \right|, \quad (16)$$

Meson/Parameters	l_z	\mathcal{N}_M	Λ_1	Λ_2	α	β
$\pi(u\bar{d})$	0	13.53 ± 2.05	1.00 ± 0.01	1.00 ± 0.01	0.51 ± 0.08	0.51 ± 0.08
	1	47.08 ± 8.07	1.26 ± 0.01	1.26 ± 0.01	0.89 ± 0.10	0.89 ± 0.10
$K(s\bar{u})$	0	24.60 ± 0.75	1.20 ± 0.01	1.03 ± 0.01	1.19 ± 0.07	$0.60 + 0.07$
	1	85.77 ± 13.09	1.20 ± 0.02	$1.18 + 0.01$	1.37 ± 0.13	$1.14 + 0.08$
$D_u(c\bar{u})$	0	5.82 ± 1.03	$2.13 + 0.06$	1.06 ± 0.03	-0.29 ± 0.18	-1.84 ± 0.12
	1	16.89 ± 3.46	1.89 ± 0.08	1.20 ± 0.03	1.10 ± 0.20	-2.47 ± 0.16
$D_s(c\bar{s})$	0	3.01 ± 1.00	2.08 ± 0.11	1.38 ± 0.06	-1.41 ± 0.35	-1.85 ± 0.21
	1	5.90 ± 0.73	1.85 ± 0.18	1.69 ± 0.07	-0.33 ± 0.13	-2.36 ± 0.11
$\eta_c(c\bar{c})$	0	0.17 ± 0.06	2.19 ± 0.04	2.19 ± 0.04	-5.53 ± 0.40	0.00
	1	6.75 ± 2.22	2.11 ± 0.041	2.11 ± 0.041	-1.14 ± 0.41	0.00
$B_u(b\bar{u})$	0	10.52 ± 2.26	5.53 ± 0.14	0.99 ± 0.07	2.22 ± 0.20	-2.50 ± 0.19
	1	4.98 ± 0.50	4.79 ± 0.18	1.40 ± 0.05	4.58 ± 0.06	-4.72 ± 0.13
$B_s(b\bar{s})$	0	13.21 ± 3.45	4.86 ± 0.33	1.56 ± 0.15	1.93 ± 0.30	-2.15 ± 0.23
	1	9.91 ± 1.18	4.95 ± 0.45	1.68 ± 0.12	$4.13 + 0.32$	-4.25 ± 0.13
$B_c(b\bar{c})$	0	0.61 ± 0.23	5.17 ± 0.30	2.21 ± 0.22	-3.30 ± 0.36	-3.71 ± 0.32
	1	3.52 ± 0.90	4.91 ± 0.28	$2.32 + 0.18$	-0.69 ± 0.26	-2.61 ± 0.26
$\eta_b(b\bar{b})$	0	0.02 ± 0.01	5.47 ± 0.11	5.47 ± 0.11	-8.05 ± 0.28	0.00
	1	7.97 ± 2.41	5.28 ± 0.12	5.28 ± 0.12	$0.56 + 0.46$	0.00

TABLE I: Parameters obtained from the LFWF reconstruction via Eq. (16) for the angular momenta $l_z = 0$ and $l_z = |1|$.

and where the moments $\langle x^m \rangle_{L,H}^{\text{rec.}}$ are calculated using Eq. (6) with Eq. (14) or Eq. (15), whereas $\langle x^m \rangle_{l_z}$ denotes the \mathbf{k}_\perp^2 -dependent moments in Eq. (7). We use $m_{\text{max}} = 5$ moments in Eq. (16), which allows for a robust reconstruction. While the \mathbf{k}_\perp -dependent part of the algebraic model only takes into account the dominant amplitude of the meson BSA [15], we here assume that we can reconstruct the wave function with all scalar amplitudes of the BSA, the advantage being that in Eq. (12) the relation between the LFWF and the LFDA is simple. We verify that the LFWF of the light mesons and the heavy quarkonia can also be extracted directly from Eq. (7), that is without resorting to the above reconstruction, by performing the $dk^+ dk^-$ integration with the help of a Feynman parametrization and a suitable variable transformation [26]. However, in order to do so, a shift $k \rightarrow k - \eta P$ has to be applied to the quark momenta in Eq. (4), which becomes impractical for $P^2 \lesssim -m_D^2$, as the integration inevitably reaches poles in the quark propagators (8).

The fitted parameters are listed in Tab. I for the angular projection $l_z = 0$ and $l_z = 1$. Generally, the moments $\langle x^m \rangle_{l_z}$ are monotonously decreasing functions of \mathbf{k}_\perp^2 and tend to zero in the limit $\mathbf{k}_\perp^2 \rightarrow \infty$. They are, moreover, suppressed with increasing values of m . The LFWFs of the mesons we consider are plotted in Fig. 1 for $l_z = 0$. For $|l_z| = 1$ they can be readily obtained from Eq. (12) and Tab. I. As expected, $\Lambda_1 = \Lambda_2$ and $\alpha = \beta$ for equal-mass mesons, whereas one has $\Lambda_1 \neq \Lambda_2$ and $\alpha \neq \beta$ for flavored mesons. In case of the light mesons, we observe that at large \mathbf{k}_\perp^2 the LFWFs decay as $\psi_0(x, \mathbf{k}_\perp^2) \sim 1/\mathbf{k}_\perp^2$ and $\psi_1(x, \mathbf{k}_\perp^2) \sim 1/\mathbf{k}_\perp^4$, in agreement with perturbative QCD [27], and the wave functions reflects the dynamical chiral symmetry breaking properties of the Bethe-Salpeter wave functions. That is, their x -dependence is broad at low \mathbf{k}_\perp^2 and narrows as \mathbf{k}_\perp^2 increases, ap-

proaching the asymptotic form $x(1-x)$. The effect of SU(3) flavor symmetry breaking is clearly visible for the kaon, as the heavier strange quark gains more support at larger x and the LFWF is skewed. This observation is exacerbated for charm and bottom mesons with a strong shift to larger x of the heavy quark's support, whereas a ridge forms along \mathbf{k}_\perp^2 with increasing meson mass. Their LFWFs decay at larger \mathbf{k}_\perp^2 , in particular those of the η_c and η_b quarkonia.

So far, we have not discussed the scale dependence of the LFWF. Since we use a model for the gluon interaction [18, 21] in ladder truncation, the renormalization scale of the quark propagators $S_f(k)$ is not that in a given scheme in perturbative QCD. We therefore determine the scale with the experimental value of the the momentum fraction carried by the valence quarks from a πN Drell-Yan analysis, $2\langle x \rangle_v = 0.47(2)$ at a scale of $Q^2 = 4 \text{ GeV}^2$ [28, 29]. By solving the NLO DGLAP evolution equations numerically with QCDNUM [30] we determine our model scale to be $Q_0 = 0.53 \text{ GeV}$.

III. DISTRIBUTION FUNCTIONS

With the meson's LFWF at hand one can readily derive three distributions. The leading-twist distribution amplitude of the meson is obtained by integrating over the quark's transverse momentum [1],

$$\phi_M(x) = \frac{1}{16\pi^3} \int^{\Lambda_\perp^2} \Psi_0(x, \mathbf{k}_\perp^2) d^2\mathbf{k}_\perp, \quad (17)$$

normalized with weak decay constant f_M ,

$$\int_0^1 \phi_M(x) dx = f_M. \quad (18)$$

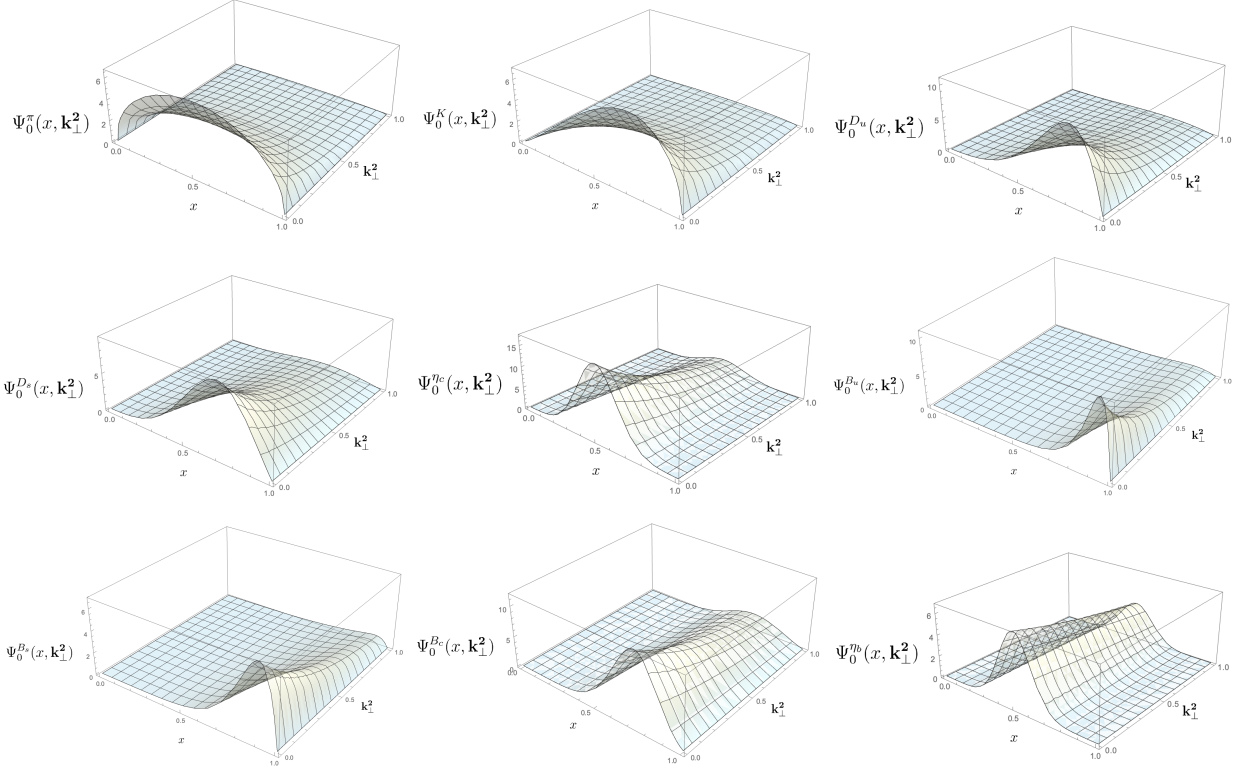


FIG. 1: Light-front wave functions of light and heavy pseudoscalar mesons for the angular projection $l_z = 0$ reconstructed from transverse-momentum dependent moments $\langle x^m \rangle_{l_z}(\mathbf{k}_\perp^2)$ at the scale $Q_0 = 0.53$ GeV.

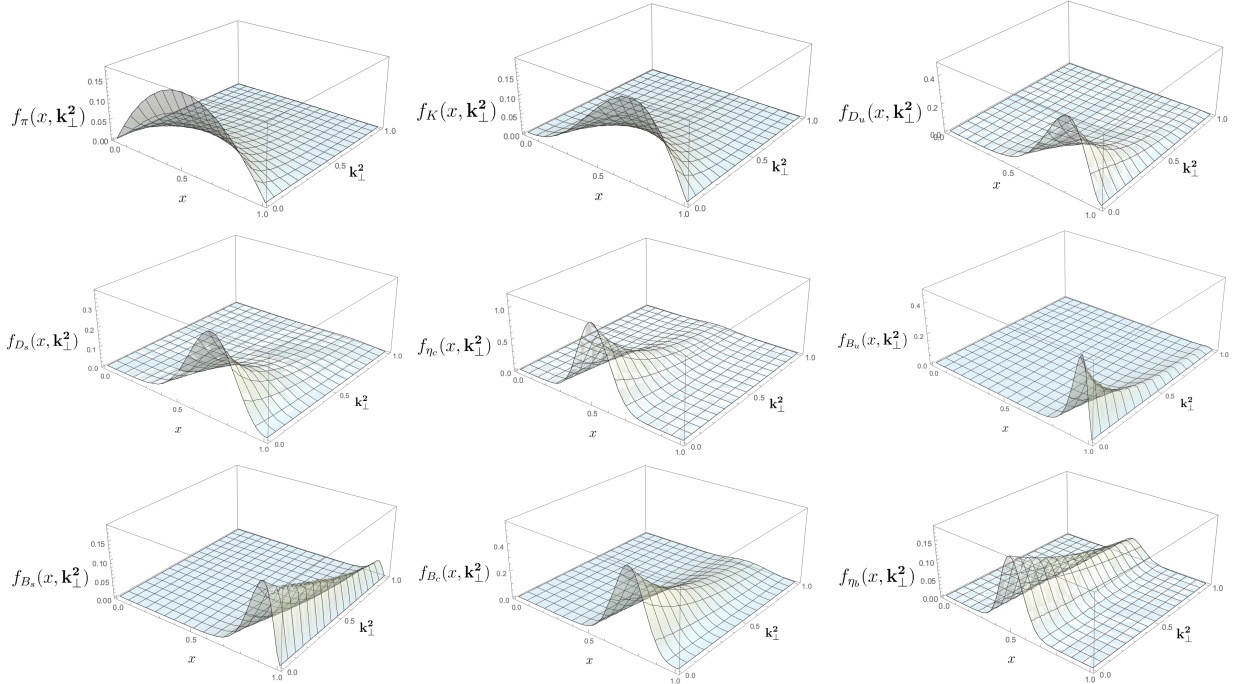


FIG. 2: Transverse momentum distributions of pseudoscalar mesons for the minimal Fock-state configuration in Eq. (19) at the scale $Q_0 = 0.53$ GeV.

The leading-twist time-reversal even TMD is given in terms of the minimal Fock-state LFWFs as [4, 31],

$$f_M(x, \mathbf{k}_\perp^2) = \frac{1}{(2\pi)^3} \left(|\Psi_0(x, \mathbf{k}_\perp^2)|^2 + \mathbf{k}_\perp^2 |\Psi_1(x, \mathbf{k}_\perp^2)|^2 \right), \quad (19)$$

and the PDF is obtained therefrom by integrating over the quark's transverse momentum:

$$q_M(x, Q_0) = \int^{\Lambda_\perp^2} f_M(x, \mathbf{k}_\perp^2) d^2 \mathbf{k}_\perp. \quad (20)$$

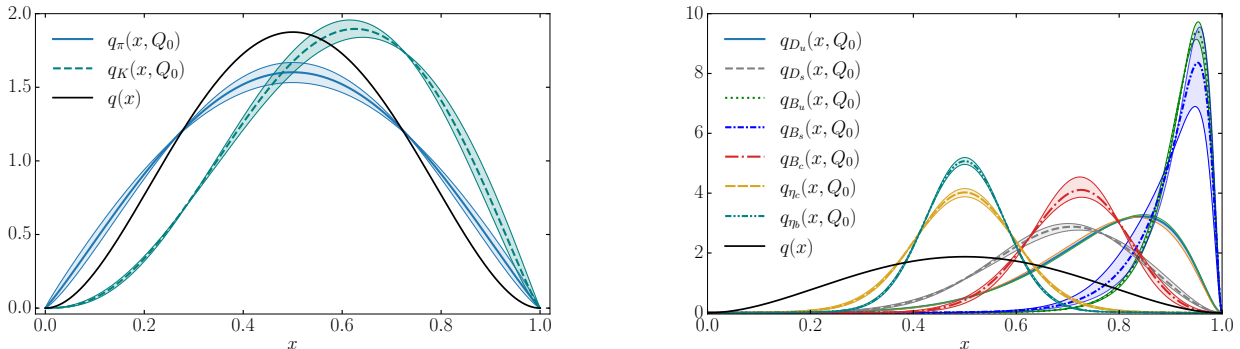


FIG. 3: Parton distribution functions of light and heavy mesons calculated at the scale $Q_0 = 0.53 \text{ GeV}$. For comparison, the asymptotic form $q(x) \sim [x(1-x)]^2$ is plotted. The error bands are due to the reconstruction procedure and stem from the uncertainties in the parameters \mathcal{N}_M , α , β , Λ_1 and Λ_2 in Eq. (12).

The normalization condition that guarantees baryon number conservation of the LFWF is:

$$\int_0^1 q_M(x, Q_0) dx = 1. \quad (21)$$

In Fig. 2, the unpolarized TMDs of the pseudoscalar mesons are presented as functions of \mathbf{k}_\perp^2 and x . We point out that this includes the first TMD calculation of D and B mesons within the DSE-BSE approach. The transverse distributions mirror the functional behavior of the LFWF discussed in Sec. II. They are smooth functions that decay with increasing \mathbf{k}_\perp^2 and as functions of x . The inflection point from a concave to a convex function of \mathbf{k}_\perp is located at about 300 MeV in the case of the pion and kaon, as was already observed in Ref. [12], and appears to persist at a similar scale even for the D , B , η_c and η_b . However, the falling off with \mathbf{k}_\perp^2 of the TMD of these mesons is significantly attenuated and their x -dependence is narrow. The latter observation is consistent with the fact that dynamical chiral symmetry breaking is less important in heavy mesons. We remind that the x -dependence of the TMDs in Eq. (12) does not factorize.

We conclude this section with the presentation of the PDFs in Fig. 3 which we obtain from the TMDs via Eq. (20) with $\Lambda_\perp^2 = 8 \text{ GeV}^2$ and the results remain unchanged for values $\Lambda_\perp^2 \geq 8 \text{ GeV}^2$. All the PDFs in Fig. 3 can be fitted with the Gegenbauer expansion,

$$q(x, Q_0) = 30 [x(1-x)]^2 \left[1 + \sum_{j=1}^{j_m} a_j C_j^{5/2}(2x-1) \right]. \quad (22)$$

We find that all the PDFs can be parametrized with $j_m = 17$. For mesons composed of the same valence quarks, only even Gegenbauer polynomials contribute to the parameterization. On the left-hand side of Fig. 3, the PDFs of the pion and kaon are compared to the asymptotic form of Eq. (22), $q(x, Q_0) = 30[x(1-x)]^2$, in the limit $Q_0 \rightarrow \infty$. We note again a clear broadening of

the distributions which is nothing but a manifestation of dynamical chiral symmetry breaking in the meson's Bethe-Salpeter wave function. Likewise, SU(3) breaking is apparent and the strange quark carries a larger fraction of the kaon's longitudinal light-front momentum. On the right-hand side of Fig. 3 the PDFs of heavy quarkonia and heavy-light mesons are shown. Their functional behavior is analogous to that observed for their distribution amplitudes, see for example Refs. [18, 20]: with increasing quark masses, the distribution functions become narrower and in case of an infinitely heavy quarkonia, one expects $q(x) \simeq \delta(x)$. The support of the D -meson distributions is shifted to larger x , even more so for the B mesons as is clear from comparison with the asymptotic distribution $q(x)$.

In Fig. 4 we show our results for the pion valence distribution v^π (multiplied by Bjorken x) as a function of x . We evolve our results at $Q_0 = 0.53 \text{ GeV}$ to a scale of $Q = 4 \text{ GeV}$ using the NLO DGLAP equations of the QCD evolution program QCDNUM [30] to compare with the LO analysis result [32]. Finally, the valence distribu-

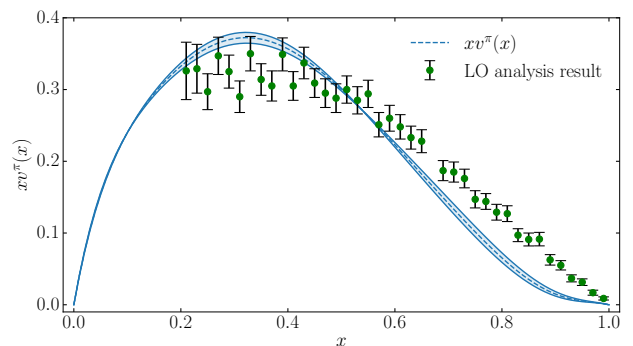


FIG. 4: Evolved pion valence PDF at $Q = 4 \text{ GeV}$ compared with the LO analysis result [32].

tion function can be very accurately parametrized with a Chebyshev expansion, as follows:

$$xv^\pi = N_v x(1-x) \left[1 + \sum_{n=1}^6 b_n U_n(2x-1) \right]. \quad (23)$$

IV. FINAL REMARKS

We projected Bethe-Salpeter wave function of pseudoscalar mesons on the light front by computing k_\perp^2 -dependent moments of the leading Fock-state LFWF, where the wave functions employed are computed in an improved ladder kernel that accounts the flavor difference of the light and heavy quarks [18]. The LFWF (2) and TMD (19) of pseudoscalar mesons we obtain provide an insightful picture of their longitudinal momentum fraction and transverse momentum dependences as a function of the quark-antiquark mass difference.

We reproduce earlier DSE-BSE calculations of the TMDs for the pion and kaon [11, 14] and for heavy quarkonia [13] and report the first TMD and PDF of D_u, D_s, B_u, B_s and B_c mesons using a functional approach. Not surprising, and mirroring the behavior of the distribution amplitudes [18, 20], the larger the quark-mass difference, the narrower the LFWF, TMD and PDF become and the more they are skewed towards larger x . Moreover, with increasing meson mass, the TMDs fall off much slower than those of the pion and kaon as a function

of k_\perp^2 . One therefore ought to be aware of this behavior when studying the transverse-momentum dependence heavy meson production amplitudes. Finally, we determine our model scale by evolving the pion valence quark distribution function to experimental scale.

Acknowledgments

We would like to acknowledge Chao Shi for the insightful discussions and for providing the PDF evolution code. F.E.S. gratefully acknowledges the EIC Theory Institute at BNL for their financial support during his research stay. B.E. and G.K. participate in the Brazilian network project *INCT-Física Nuclear e Aplicações*, grant no. 464898/2014-5. This work was supported by the São Paulo Research Foundation (FAPESP), grant no. 2023/00195-8 (B.E.) and no. 2018/25225-9 (G.K.), and by the National Council for Scientific and Technological Development (CNPq), grant no. 409032/2023-9 and no. 309262/2019-4 (G.K.).

Appendix A: Bethe-Salpeter Amplitude Parameters

In Table II we list all the parameters associated with BSA of the pseudoscalar mesons. The corresponding parametrization is detailed in Eq. (9).

-
- [1] S. J. Brodsky, H. C. Pauli and S. S. Pinsky, Phys. Rept. **301**, 299-486 (1998) doi:10.1016/S0370-1573(97)00089-6
- [2] R. L. Jaffe, [arXiv:hep-ph/9602236 [hep-ph]].
- [3] M. Burkardt, X. d. Ji and F. Yuan, Phys. Lett. B **545**, 345-351 (2002) doi:10.1016/S0370-2693(02)02596-0
- [4] B. Pasquini and P. Schweitzer, Phys. Rev. D **90**, no.1, 014050 (2014) doi:10.1103/PhysRevD.90.014050
- [5] A. Metz and A. Vossen, Prog. Part. Nucl. Phys. **91**, 136-202 (2016) doi:10.1016/j.pnpnp.2016.08.003
- [6] H. C. Pauli and S. J. Brodsky, Phys. Rev. D **32**, 2001 (1985)
- [7] J. P. Vary, H. Honkanen, J. Li, P. Maris, S. J. Brodsky, A. Harindranath, G. F. de Teramond, P. Sternberg, E. G. Ng and C. Yang, Phys. Rev. C **81**, 035205 (2010) doi:10.1103/PhysRevC.81.035205
- [8] X. Ji and Y. Liu, Phys. Rev. D **105**, no.7, 076014 (2022) doi:10.1103/PhysRevD.105.076014
- [9] C. Mezrag, H. Moutarde and J. Rodríguez-Quintero, Few Body Syst. **57**, no.9, 729-772 (2016) doi:10.1007/s00601-016-1119-8
- [10] A. Bashir, L. Chang, I. C. Cloët, B. El-Bennich, Y. X. Liu, C. D. Roberts and P. C. Tandy, Commun. Theor. Phys. **58**, 79-134 (2012) doi:10.1088/0253-6102/58/1/16
- [11] C. Shi and I. C. Cloët, Phys. Rev. Lett. **122**, no.8, 082301 (2019) doi:10.1103/PhysRevLett.122.082301
- [12] C. Shi, K. Bednar, I. C. Cloët and A. Freese, Phys. Rev. D **101**, no.7, 074014 (2020) doi:10.1103/PhysRevD.101.074014
- [13] W. Kou, C. Shi, X. Chen and W. Jia, Phys. Rev. D **108**, no.3, 036021 (2023) doi:10.1103/PhysRevD.108.036021
- [14] C. Shi, J. Li, P. L. Yin and W. Jia, Phys. Rev. D **107**, no.7, 074009 (2023) doi:10.1103/PhysRevD.107.074009
- [15] B. Almeida-Zamora, J. J. Cobos-Martínez, A. Bashir, K. Raya, J. Rodríguez-Quintero and J. Segovia, Phys. Rev. D **109**, no.1, 014016 (2024) doi:10.1103/PhysRevD.109.014016
- [16] E. Rojas, B. El-Bennich and J. P. B. C. de Melo, Phys. Rev. D **90**, 074025 (2014) doi:10.1103/PhysRevD.90.074025
- [17] F. F. Mojica, C. E. Vera, E. Rojas and B. El-Bennich, Phys. Rev. D **96**, no.1, 014012 (2017) doi:10.1103/PhysRevD.96.014012
- [18] F. E. Serna, R. C. da Silveira, J. J. Cobos-Martínez, B. El-Bennich and E. Rojas, Eur. Phys. J. C **80**, no.10, 955 (2020) doi:10.1140/epjc/s10052-020-08517-3
- [19] F. E. Serna and B. El-Bennich, PoS **CHARM2020**, 047 (2021) doi:10.22323/1.385.0047
- [20] F. E. Serna, R. C. da Silveira and B. El-Bennich, Phys. Rev. D **106**, no.9, L091504 (2022) doi:10.1103/PhysRevD.106.L091504
- [21] R. C. da Silveira, F. E. Serna and B. El-Bennich, Phys. Rev. D **107**, no.3, 034021 (2023) doi:10.1103/PhysRevD.107.034021

TABLE II: Parameters of the spectral representation of the meson's BSA (9). (Dimensioned quantities in GeV).

	Λ	U_1	U_2	U_3	n_1	n_2	n_3	σ_1	σ_2	σ_3
E_π	1.42	0.75	1.45	-1.21	4	5	6	0.00	1.13	0.00
F_π	1.43	-0.44	0.94	0.01	3	4	1	0.00	-1.30	0.00
G_π	0.80	-0.05	0.04	0.01	4	5	1	38.00	2.81	1.25
E_K	1.33	2.36	-1.09	-0.27	4	5	6	-0.97	1.28	-1.53
F_K	1.56	-0.39	0.80	0.01	3	4	1	-0.64	-1.09	1.20
G_K	1.57	0.00	0.25	-0.25	5	6	5	-1.64	2.34	-3.18
E_{η_c}	1.84	2.08	-1.13	0.06	4	5	1	0.0	-1.65	0.00
F_{η_c}	2.55	-0.02	0.15	0.00	4	6	1	0.0	-2.14	0.00
G_{η_c}	2.71	0.82	-0.08	-1.12	8	12	8	-0.33	0.00	0.75
E_{η_b}	3.31	0.16	0.78	0.06	4	5	1	0.00	-2.22	0.00
F_{η_b}	3.50	0.00	0.05	0.00	4	6	1	0.00	-2.30	0.00
G_{η_b}	3.86	0.08	-0.04	-1.54	8	12	8	-1.00	0.00	3.08
E_{D_u}	1.44	2.49	-1.50	0.01	4	5	1	0.133	-1.48	0.57
F_{D_u}	2.03	-0.07	0.278	0.00	4	6	1	-0.41	-1.92	0.90
G_{D_u}	-2.60	0.14	0.20	-0.36	8	12	8	-1.09	-1.63	2.23
E_{D_s}	1.56	2.44	-1.45	0.01	4	5	1	0.23	-1.40	0.15
F_{D_s}	1.47	0.33	-0.12	0.00	4	6	1	0.30	-1.88	-0.72
G_{D_s}	-1.50	-0.19	0.12	0.00	4	5	1	3.25	0.95	-5.07
E_{B_u}	1.55	2.61	-1.60	-0.03	4	5	1	0.13	-2.29	-0.28
F_{B_u}	2.36	-0.05	0.14	0.00	4	6	1	0.34	-2.30	-1.04
G_{B_u}	2.16	0.142	-0.01	-0.21	5	6	4	-1.36	-0.98	4.26
E_{B_s}	1.71	2.36	-1.31	-0.05	4	5	1	0.55	-2.11	-1.55
F_{B_s}	2.21	-0.01	0.10	0.00	4	6	1	0.60	-2.17	-1.83
G_{B_s}	1.58	-0.41	0.26	0.00	4	5	1	1.35	-1.57	-3.80
E_{B_c}	2.14	1.94	-0.96	0.02	4	5	1	0.33	-2.13	-0.88
F_{B_c}	2.78	0.00	0.07	0.00	4	6	1	0.33	-2.25	-0.99
G_{B_c}	2.45	0.01	0.00	0.05	5	6	4	-43.57	4.04	127.57

- [22] C. H. Llewellyn-Smith, *Annals Phys.* **53**, 521-558 (1969) doi:10.1016/0003-4916(69)90035-9
- [23] F. E. Serna, C. Chen and B. El-Bennich, *Phys. Rev. D* **99**, no.9, 094027 (2019) doi:10.1103/PhysRevD.99.094027
- [24] M. Bhagwat, M. A. Pichowsky and P. C. Tandy, *Phys. Rev. D* **67**, 054019 (2003) doi:10.1103/PhysRevD.67.054019
- [25] B. El-Bennich, G. Krein, E. Rojas and F. E. Serna, *Few Body Syst.* **57**, no.10, 955-963 (2016) doi:10.1007/s00601-016-1133-x
- [26] C. Mezrag, 2015PA112144.
- [27] X. d. Ji, J. P. Ma and F. Yuan, *Phys. Rev. Lett.* **90**, 241601 (2003) doi:10.1103/PhysRevLett.90.241601
- [28] P. J. Sutton, A. D. Martin, R. G. Roberts and W. J. Stirling, *Phys. Rev. D* **45**, 2349-2359 (1992) doi:10.1103/PhysRevD.45.2349
- [29] M. Gluck, E. Reya and I. Schienbein, *Eur. Phys. J. C* **10**, 313-317 (1999) doi:10.1007/s100529900124
- [30] M. Botje, *Comput. Phys. Commun.* **182**, 490-532 (2011) doi:10.1016/j.cpc.2010.10.020
- [31] W. de Paula, E. Ydrefors, J. H. Nogueira Alvarenga, T. Frederico and G. Salmè, *Phys. Rev. D* **105**, no.7, L071505 (2022) doi:10.1103/PhysRevD.105.L071505
- [32] J. S. Conway, C. E. Adolphsen, J. P. Alexander, K. J. Anderson, J. G. Heinrich, J. E. Pilcher, A. Possoz, E. I. Rosenberg, C. Biino and J. F. Greenhalgh, *et al.* *Phys. Rev. D* **39** (1989), 92-122 doi:10.1103/PhysRevD.39.92